18th International Conference
ENGINEERING MECHANICS 2012
Svratka, Czech Republic, May 14 – 17, 2012

pp. 345–353
Paper #138

NUMERICAL SIMULATION OF TWO-PHASE FLOW IN A LOW PRESSURE STEAM TURBINE STAGE

J. Halama *, **J. Fořt** **

Abstract: *The paper deals with the numerical solution of two phase unsteady flow in a steam turbine stage performed by in-house numerical code. The main issues related to the flow model, numerical method and problem formulation are presented. The effect of droplet size of incoming wet steam is discussed.*

Keywords: ***Finite volume method, turbine, nucleation, wet steam, CFD.***

1. Introduction

The paper presents the results of recent work aimed at the simulation of steam flow with non-zero wetness at the inlet. The problem formulation requires the complete information about the structure of incoming liquid phase. It is relatively easy to estimate the inlet wetness, however the flow models have other unknowns, which have to be set. The presented model is based on the transport equations for three moments. The values of these moments for the inlet boundary condition have been estimated using numerical simulation of upstream expansion. Numerical test have shown, that numerical solution is quite sensitive to the given values of moments. This phenomenon has been studied for the steady flow in the nozzle. Similar effects have been observed in the case of unsteady flow in a turbine stage.

2. Flow model

Consider the flow of steam with velocity, pressure and temperature corresponding to the conditions within the low pressure part of a steam turbine. The rapid expansion of steam leads to non-equilibrium phase change, i.e. the condensation appears 'later', when the steam temperature drops sufficiently below the saturation temperature. This 'sub-cooling' is typically $30 - 40\ K$. Consider the liquid phase in the form of high amount of small spherical droplets dispersed in vapor and having the same velocity as the vapor. There is a mass exchange between vapor and droplets due to phase change. The flow model is based on the conservation of mass, momentum and energy for the mixture and the transport equation for the mass fraction of liquid phase. Such kind of model, known also as 'mixture model', is commonly used, e.g. Dykas et al (2003), Young (1992) or Šejna and Lain (1994). The droplet size is an important parameter. In reality there is a whole spectra of droplet sizes in the elemental volume of mixture. Flow models are mostly based on the average radius approximation, therefore the mentioned set of transport equations has to be complemented at least by the transport equation for the number of droplets, e.g. Dykas et al (2003). Here we consider three additional transport equations for the moments according to Hill (1966) to obtain higher precision of average droplet size prediction and to be able to add some simple model of droplet size distribution, for details see Halama et al (2010). The moments read:

$$Q_0 = N, \qquad Q_1 = \sum_{i=1}^{N} r_i, \qquad Q_2 = \sum_{i=1}^{N} r_i,^2 \tag{1}$$

*Jan Halama: Department of Technical Mathematics, Faculty of Mechanical Engineering, Czech Technical University in Prague, Karlovo nam. 13, 121 35, Prague; CZ, e-mail: jan.halama@fs.cvut.cz
**Jaroslav Fořt: Department of Technical Mathematics, Faculty of Mechanical Engineering, Czech Technical University in Prague, Karlovo nam. 13, 121 35, Prague; CZ, e-mail: jaroslav.fort@fs.cvut.cz

where N denotes the total number of droplets per unit mass and r_i is the radius of $i-th$ droplet. The average droplet radius is approximated by $r = \sqrt{Q_2/Q_0}$. The full system of transport equations reads

$$\frac{\partial \mathbf{W}}{\partial t} + \frac{\partial \mathbf{F}(\mathbf{W})}{\partial x} + \frac{\partial \mathbf{G}(\mathbf{W})}{\partial y} = \mathbf{Q}, \tag{2}$$

$$\mathbf{W} = \begin{bmatrix} \rho \\ \rho u \\ \rho v \\ e \\ \rho\chi \\ \rho Q_2 \\ \rho Q_1 \\ \rho Q_0 \end{bmatrix}, \mathbf{F} = \begin{bmatrix} \rho u \\ \rho u^2 + p \\ \rho uv \\ (e+p)u \\ \rho\chi u \\ \rho Q_2 u \\ \rho Q_1 u \\ \rho Q_0 u \end{bmatrix}, \mathbf{G} = \begin{bmatrix} \rho v \\ \rho vu \\ \rho v^2 + p \\ (e+p)v \\ \rho\chi v \\ \rho Q_2 v \\ \rho Q_1 v \\ \rho Q_0 v \end{bmatrix}, \mathbf{Q} = \begin{bmatrix} 0 \\ 0 \\ 0 \\ 0 \\ \frac{4}{3}\pi r_c^3 J\rho_l + 4\pi\rho Q_2 \dot{r}\rho_l \\ r_c^2 J + 2\rho Q_1 \dot{r} \\ r_c J + \rho Q_0 \dot{r} \\ J \end{bmatrix},$$

where ρ, u, v and e denotes the mixture density, velocity components and total energy per unit volume respectively. The symbol χ denotes the mass fraction of liquid phase (wetness). Under the perfect gas assumption the system is closed by the equation

$$p = \frac{(\gamma-1)(1-\chi)}{1+\chi(\gamma-1)}\left[e - \frac{1}{2}\rho(u^2+v^2) + \rho\chi L\right], \tag{3}$$

for further details see Šejna and Lain (1994) and Halama et al (2011). The common pressure for both phases is considered. The system (2) turns into the 2D Euler equations for the one phase flow if liquid phase vanishes ($\chi = Q_0 = Q_1 = Q_2 = 0$).

The specific heat ratio reads

$$\gamma = \frac{c_p}{c_p - R_v}, \tag{4}$$

where R_v is the gas constant for vapor and the specific heat at constant pressure c_p is a function of temperature in form

$$c_p = c_0 + c_1 T + c_2 T^2 + c_3 T^3. \tag{5}$$

According to the perfect gas assumption the vapor temperature

$$T = \frac{p}{\rho_v R_v}, \quad \rho_v = (1-\chi)\rho. \tag{6}$$

The number of suddenly born droplets per second in unit volume is given by the nucleation rate according to classical theory in Becker and Doering (1935)

$$J = \sqrt{\frac{2\sigma}{\pi m_v^3}} \cdot \frac{\rho_v^2}{\rho_l} \cdot \exp\left(-\beta \cdot \frac{4\pi r_c^2 \sigma}{3k_B T}\right) \qquad [m^{-3}s^{-1}], \tag{7}$$

where the surface tension σ of water is a function of temperature and it is corrected by the coefficient β proposed in Petr and Kolovratník (2001) to get better agreement with reality

$$\beta = 1.328 p_{cor}^{0.3}, \tag{8}$$

where p_{cor} $[bar]$ denotes the pressure at the intersection of the isentropic expansion from reservoir conditions (p_0 and T_0) with the steam saturation line in the Mollier diagram, see the Fig. 1. The just born droplet has radius equal to the critical radius

$$r_c = \frac{2\sigma}{L\rho_l \ln(T_s/T)} \qquad [m], \tag{9}$$

where $L(T)$ is the latent heat of condensation/evaporation and $\rho_l(T)$ denotes the density of water. The saturation temperature T_s is computed using industrial formulation of steam properties IAPWS-IF97. Droplet growth is computed as

$$\dot{r} = \frac{\lambda_v(T_s - T)}{L\rho_l(1 + 3.18 \cdot Kn)} \cdot \frac{r - r_c}{r^2} \qquad [ms^{-1}], \tag{10}$$

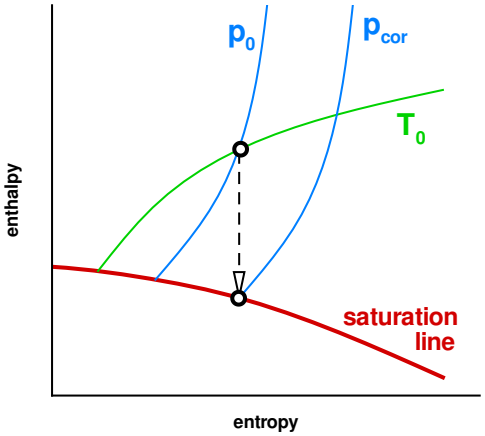

Fig. 1: Definition of p_{cor}.

with

$$Kn = \frac{\eta_v \cdot \sqrt{2\pi R_v T}}{4rp} \tag{11}$$

where vapor thermal conductivity λ_v and vapor viscosity η_v are functions of temperature.

We consider a certain limit value χ_{min} for wetness in order to avoid big computational errors (e.g. division by numbers going to zero, ...). The average radius is therefore computed as

$$r = \begin{cases} 0, & \chi \leq \chi_{min}, \\ \sqrt{Q_2/Q_0}, & \chi > \chi_{min}. \end{cases} \tag{12}$$

Flow models based on the average size of droplets may not work properly in certain conditions, therefore according to Sopuch (1996) we split the evaluation of source term **Q** into four cases

1. $T \geq T_s$ and $r \leq r_{min}$: all droplets have disappeared, i.e. set $\chi = Q_0 = Q_1 = Q_2 = 0$
2. $T \geq T_s$ and $r > r_{min}$: droplets are evaporating, set $r_c = 0$ in Eq. (10)
3. $T < T_s$ and $r \leq r_c$: consider nucleation only, set $\dot{r} = 0$
4. $T < T_s$ and $r > r_c$ nucleation and droplet growth according to the above formulas

The value of r_{min} is chosen appropriately.

There can be a problem with direct evaluation of droplet growth speed according to the Eq. (10), since the critical radius goes to infinity, when the vapor temperature approaches the saturation temperature. From the mathematical point of view this growth is controlled by the term $(T_s - T)$, which is going to zero at the same time, so the droplet growth speed $\dot{r}$ remains finite. However direct implementation of the Eq. (10) in the numerical code is dangerous, since the product of 'almost infinity' with 'almost zero' has unpredictably unstable behavior. Therefore we consider both equations (9) and (10) together in the form

$$\dot{r} = \frac{\lambda_v (T_s - T)}{L\rho_l (1 + 3.18 \cdot Kn)} \frac{r - r_c}{r^2} = \frac{\lambda_v}{L\rho_l (1 + 3.18 \cdot Kn)} \left(\frac{T_s - T}{r} - \frac{2\sigma}{L\rho_l r^2} \cdot \frac{T_s - T}{\ln \frac{T_s}{T}} \right), \tag{13}$$

where the term $\dfrac{T_s - T}{\ln \frac{T_s}{T}}$ ('zero' divided by 'zero' for T going to T_s) is approximated using the first six terms of Taylor expansion

$$\frac{T_s - T}{\ln \frac{T_s}{T}} = T \frac{\frac{T_s}{T} - 1}{\ln \frac{T_s}{T}} = 1 + \frac{1}{2}\vartheta - \frac{1}{12}\vartheta^2 + \frac{1}{24}\vartheta^3 - \frac{19}{720}\vartheta^4 + \frac{3}{160}\vartheta^5, \qquad \vartheta = \frac{T_s}{T} - 1. \tag{14}$$

This approximation yields stable numerical algorithm for cases with steam parameters close to saturation line.

3. Numerical method

Presented flow model includes convection, nucleation and droplet growth phenomena, which have very different time scales. Current numerical method is based on the splitting method of Strang (1968), where each phenomena is treated by individual numerical method. We use symmetrical splitting, i.e. we solve three successive equations

$$\frac{\partial \mathbf{W}^*}{\partial t} = \mathbf{Q}(\mathbf{W}^*) \tag{15}$$

$$\frac{\partial \mathbf{W}^{**}}{\partial t} = -\frac{\partial \mathbf{F}^c(\mathbf{W}^{**})}{\partial x} - \frac{\partial \mathbf{G}^c(\mathbf{W}^{**})}{\partial x} \tag{16}$$

$$\frac{\partial \mathbf{W}^{***}}{\partial t} = \mathbf{Q}(\mathbf{W}^{***}), \tag{17}$$

where $\mathbf{W}^*(t) = \mathbf{W}(t)$, $\mathbf{W}^{**}(t) = \mathbf{W}^*(t + \Delta t/2)$ and $\mathbf{W}^{***}(t) = \mathbf{W}^{**}(t + \Delta t)$. The solution $\mathbf{W}^{***}(t + \Delta t/2)$ corresponds to the solution $\mathbf{W}(t + \Delta t)$ of the original un-split system (2). The single step of Lax-Wendroff finite volume method is applied for (16) and several steps of Runge-Kutta method evaluate the source term contribution in (15) and (17). The algorithm of splitting method reads

$$\begin{aligned} \mathbf{W}_K^{(j+1)} &= \mathcal{RK}(\mathbf{W}_K^{(j)}, \frac{\Delta t}{2m}),\ j = 0, \ldots, m-1 \\ \mathbf{W}_K^{(m+1)} &= \mathcal{FV}(\mathbf{W}_K^{(m)}, \Delta t) \\ \mathbf{W}_K^{(j+1)} &= \mathcal{RK}(\mathbf{W}_K^{(j)}, \frac{\Delta t}{2m}),\ j = m+1, \ldots, 2m \end{aligned} \tag{18}$$

where $\mathbf{W}_K^{(0)} = \mathbf{W}_K^n$, $\mathbf{W}_K^{n+1} = \mathbf{W}_K^{(2m+1)}$, $\mathcal{FV}(\mathbf{W}_K^n, \Delta t)$ denotes one step of Lax-Wendroff method with initial data $\mathbf{W}_K^n$ and time step Δt (subscript $\cdot_K$ denotes the K-th cell and superscript $\cdot^n$ n-th time level). Similarly $\mathcal{RK}(\mathbf{W}_K^n, \Delta t)$ denotes one step of the Runge-Kutta method. The local number of sub-steps is $m = \Delta t/\tau$, where τ is the time scale of condensation and Δt is the time step of finite volume method for the equation (16). Domain of solution is discretized by the body fitted quadrilateral structured mesh.

4. Wet steam flow in the convergent-divergent nozzle

Current numerical method has been verified for the case of steam flow in the Barschdorff nozzle, for details see Halama et al (2011). There have been performed also computations of steam flow in a turbine cascade and turbine stage. All cases have been chosen to have steam temperature slightly below saturation temperature and zero wetness at the inlet, nucleation then starts inside the domain. Recent work has been aimed at the case of flow with nonzero wetness at the inlet. Since it is practically impossible to get reliable information about the droplet size structure of incoming steam, some basic numerical study for case of flow in a nozzle has been performed. The inlet boundary condition besides the the value of wetness requires also the values for moments, which have been estimated using numerical simulation of upstream expansion. The values of moments can be thus subjected to certain error. The following test cases investigate the sensitivity of numerical solution on the values of moments of incoming wet steam, in other words the sensitivity on the size of incoming droplets. Consider the geometry of Barschdorff nozzle from Barschdorff (1971) and three flow cases, which differ only in moments of incoming wet steam. The outflow static pressure corresponds to the design conditions of nozzle, this means supersonic velocity at the outlet and therefore no outlet boundary condition. Parameters of the flow cases are given in the Table 1.

Computed pressure, Mach number, wetness and average radius distributions along the nozzle axis are presented in the Fig. 2. The inflow droplet size in the case 1D-A is comparable to the critical radius, therefore the droplet growth given by the Eq. (13) is close to zero and the vapor sub-cooling grows til the rear part of the nozzle. The nucleation, which starts at the rear part is hardly noticeable, since the inflow vapor contains too many (too small) droplets so the number of newly born droplets does not increase much the number of already existing droplets. The wetness rise due to the nucleation is also small. If we consider bigger droplets at the nozzle inlet, see the case 1D-B, droplets gradually grow and

Tab. 1: Parameters of considered flow cases.

case	1D-A	1D-B	1D-C
$p_{0,inlet}\ [Pa]$	21061	21061	21061
$T_{0,inlet}\ [K]$	334.3	334.3	334.3
$\chi_{inlet}\ [-]$	0.349	0.349	0.349
$Q_{0,inlet}\ [kg^{-1}]$	$0.118 \cdot 10^{23}$	$0.111 \cdot 10^{19}$	$0.111 \cdot 10^{13}$
$Q_{1,inlet}\ [mkg^{-1}]$	$0.112 \cdot 10^{12}$	$0.111 \cdot 10^{11}$	$0.111 \cdot 10^{7}$
$Q_{2,inlet}\ [m^2kg^{-1}]$	$0.392 \cdot 10^{3}$	$0.111 \cdot 10^{3}$	$0.111 \cdot 10^{1}$

the sub-cooling is small, it means that local wetness is close to the local equilibrium wetness. Since the sub-cooling is small, there is no nucleation. The last case 1D-C considers the biggest droplets at the inlet. Wetness rise due to droplet growth is negligible compared to the case 1D-B since the total surface of droplets which is proportional to the second moment Q_2 is small. The vapor sub-cooling grows and downstream the throat nucleation starts, which yields significant droplet size drop. The present model with single average size of droplets is no more suitable for such case, because it is not able to distinguish two groups of droplets with very different sizes. All three cases refer to the considerable sensitivity

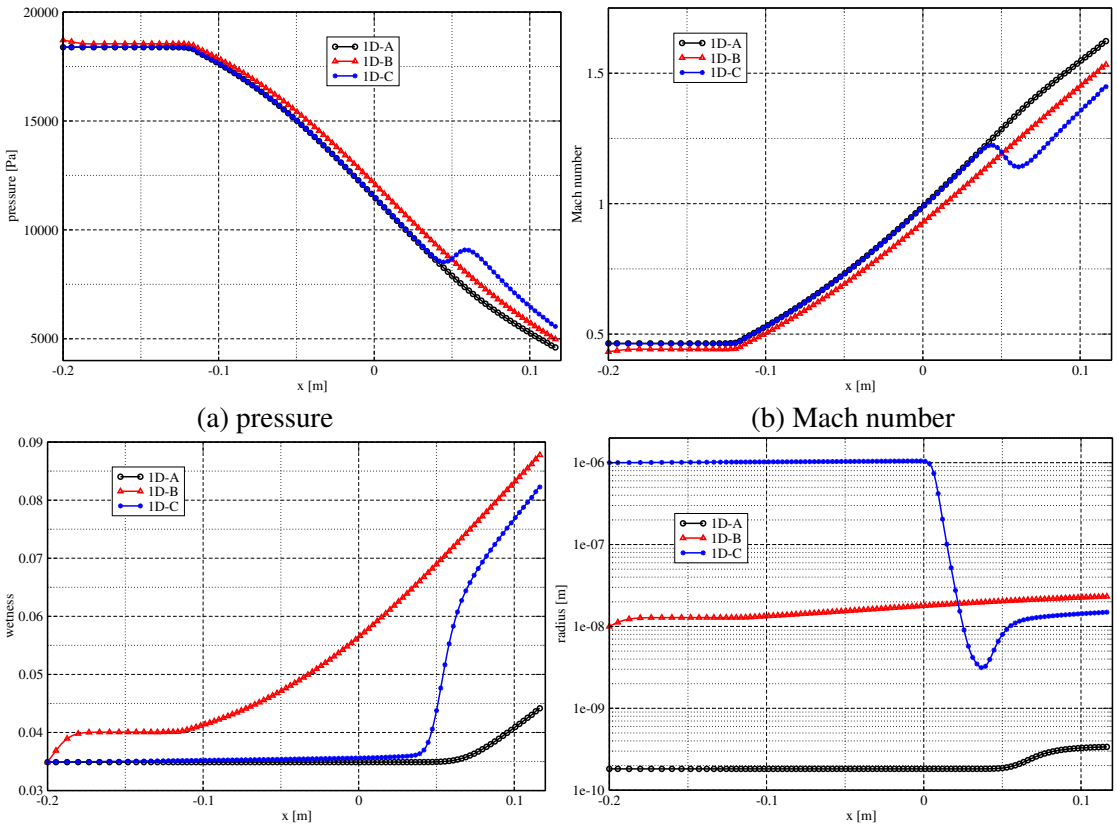

(a) pressure (b) Mach number

(c) wetness (d) droplet average radius

Fig. 2: The distributions along nozzle axis.

of condensing steam flow model on the structure of liquid phase at the inlet. Therefore one has to be very careful with the estimation of inlet boundary conditions as well as with conclusions about results of numerical simulation.

5. Stator-rotor interaction

Here we present the first results of unsteady stator-rotor interaction with the non-zero wetness at the inlet. A two-dimensional case corresponds to the cylindrical cut from the real annular stage projected onto plane. The set of equation (2) is solved in the coordinate system attached to the each respective blade cascade, i.e. in the absolute frame for stator and in the relative frame for the rotor. Numerical domain consists of 8 stator and 11 rotor blade passages to keep the original ratio of stator to rotor number of blades. Computational grid consists of single H-type structured block per each blade channel. The single stator channel is discretized by 112x45 points and the single rotor one using 141x33 points, see the Fig. 3.

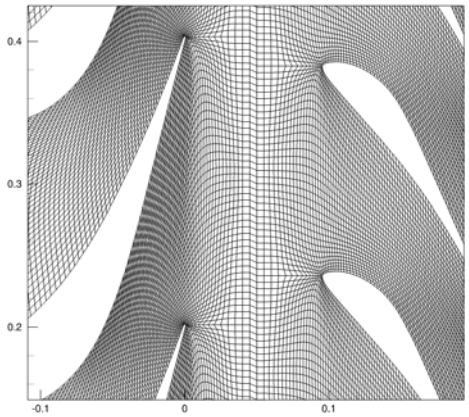

Fig. 3: Detail of computational grid at stator-rotor interface.

Initial computations have been performed for inlet boundary conditions related to the case 1D-A for the nozzle and outlet static pressure $4165\ Pa$. Numerous tests with relaxed time step, increased artificial dissipation etc. were performed to suppress the appearance of oscillations in the stator cascade. The regularization of droplet growth model, see the Eq. (13) and (14), helped to stabilize the numerical algorithm, although some oscillations of solution in the stator cascade remained, see the wetness isolines in the Fig. 4. These oscillation have most probably their origin in 'too small' size of droplets . The

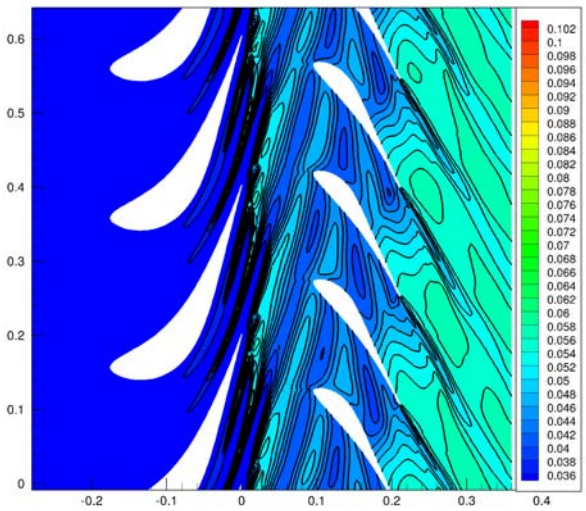

Fig. 4: Wetness contours at $t = t_0$ for 'too small' droplets at the inlet

values of moments for that case have been obtained from numerical solution in upstream stage, where

nucleation took place close to stage outlet and the numerical simulation under-predicted the size of droplets. Therefore we further present the case with 'bigger' droplets (the moments Q_i were modified).

We compare two cases. The case 1, which models only convection of wet steam, i.e. the source term including nucleation and droplet growth is omitted. The case 2 considers the solution of complete system with nucleation and droplet growth. Both cases have the same boundary conditions, the inlet boundary conditions corresponds to the case 1D-B for the nozzle in the previous section. The outlet static pressure is $4165\ Pa$. The Fig. 5 shows isolines of pressure in two consequent positions of rotor cascade during the rotor movement of one rotor pitch (the time necessary for the rotor shift of one pitch is denoted as τ_R). The flow field in the stator cascade does not contain shock waves, the pressure field between stator and rotor is without strong gradients. The structure of isolines for different rotor positions is thus very similar. The following figures 6 - 8 show isolines of wetness, vapor sub-cooling and average droplet radius respectively. These figures does not contain the results of case 1, since this case models only pure convection of vapor with parameters given by the inlet boundary conditions, i.e. the Figures 6 - 8 for the case 1 would show only a constant value everywhere.

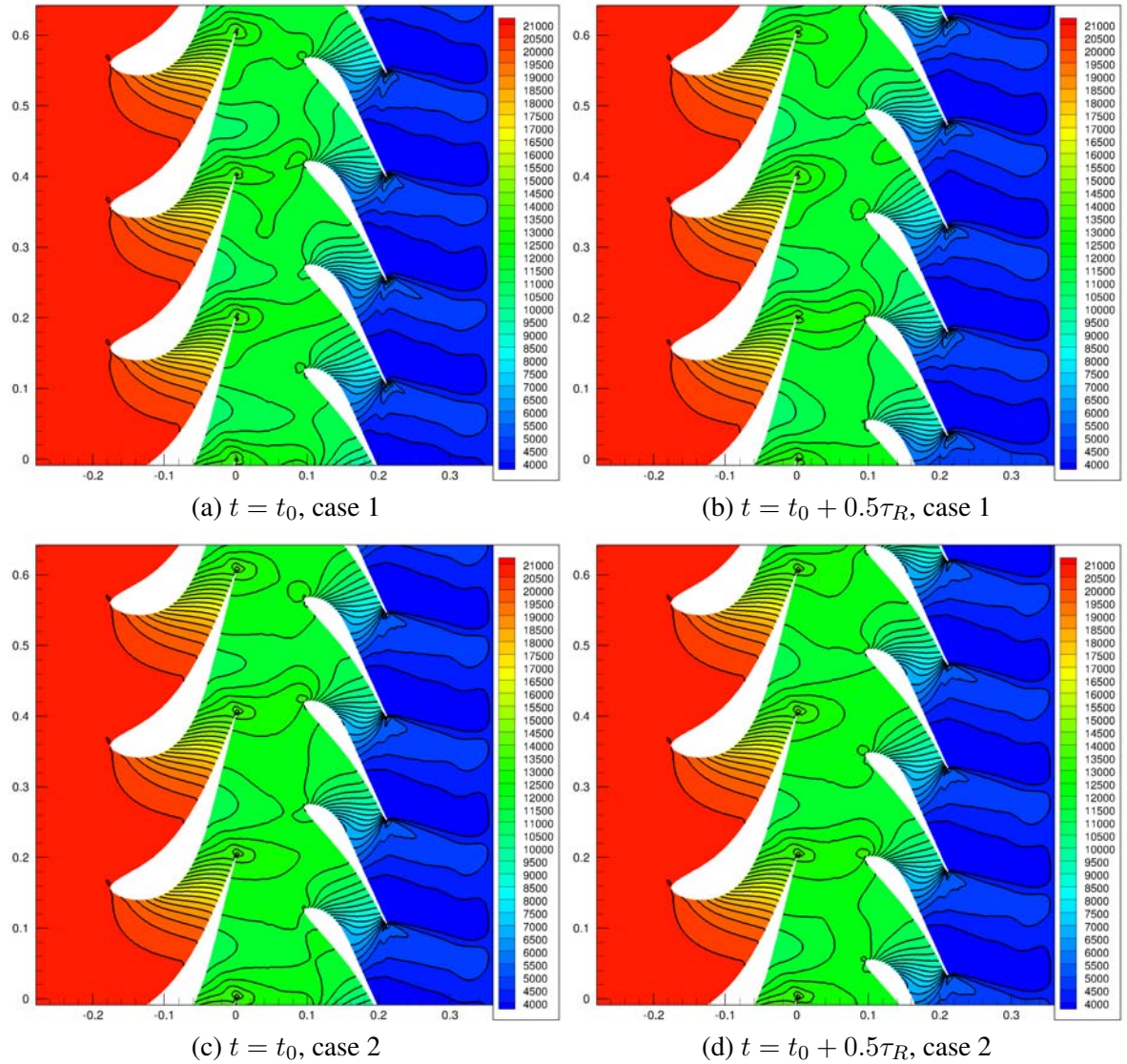

(a) $t = t_0$, case 1 (b) $t = t_0 + 0.5\tau_R$, case 1

(c) $t = t_0$, case 2 (d) $t = t_0 + 0.5\tau_R$, case 2

Fig. 5: Pressure field.

6. Conclusions

Current numerical method has been successfully extended for the cases with non-zero wetness of incoming steam. The droplet growth model has been regularized. The numerical method has stable behavior

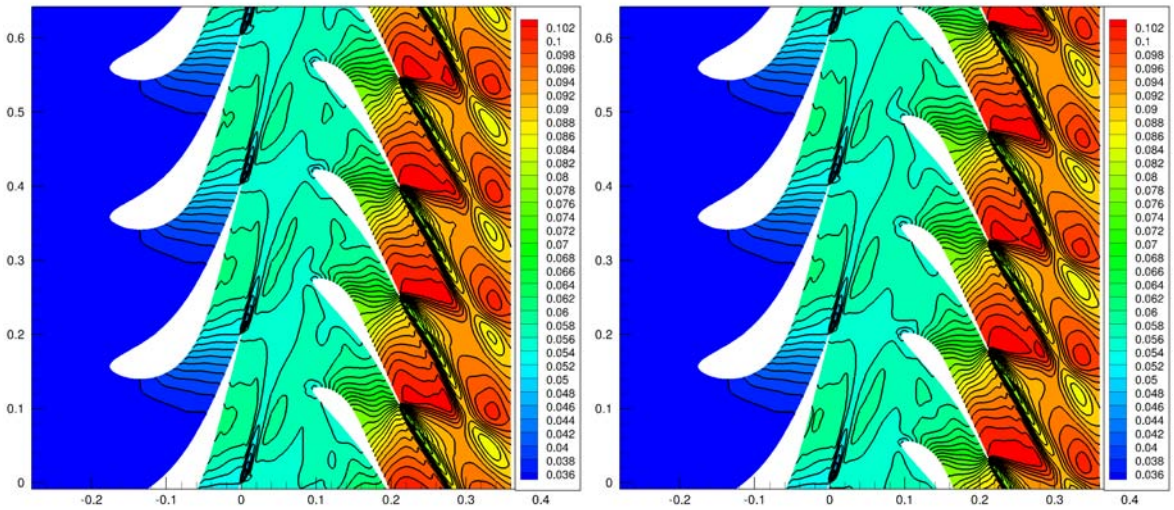

(a) $t = t_0$, case 2 (b) $t = t_0 + 0.5\tau_R$, case 2

Fig. 6: Wetness contours.

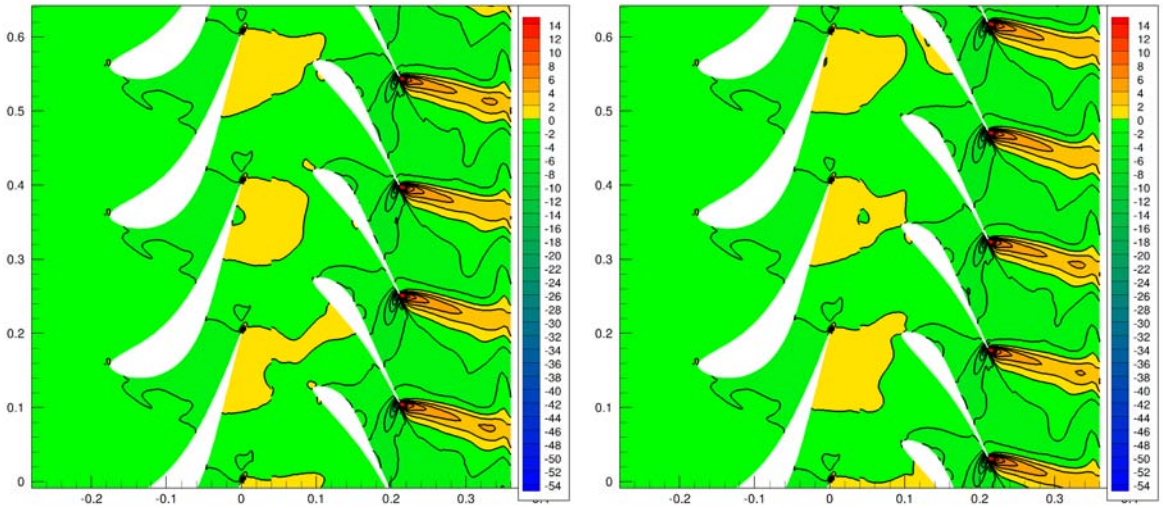

(a) $t = t_0$, case 2 (b) $t = t_0 + 0.5\tau_R$, case 2

Fig. 7: Vapor sub-cooling contours.

in the case of steady flow in a nozzle as well as unsteady flow in a turbine stage. The sensitivity of numerical results on the droplet size of incoming steam has been reported. The results achieved for cases with identical wetness and different sizes of droplets at the inlet have shown, that the droplet size has a non-negligible effect also for pressure distribution in the whole computational domain. One has to be careful with the problem formulation, since the values of moments at the inlet has to be usually estimated by numerical simulation and thus they may be deteriorated by some errors. This work showed the need for improved droplet growth model to get more reliable droplet size prediction.

Acknowledgments

This work was supported by the grant No. 101/11/1593 of Grant Agency of the Czech Republic and by the grant No. SGS10/244/OHK2/3T/12 of Grant Agency of the Czech Technical University in Prague.

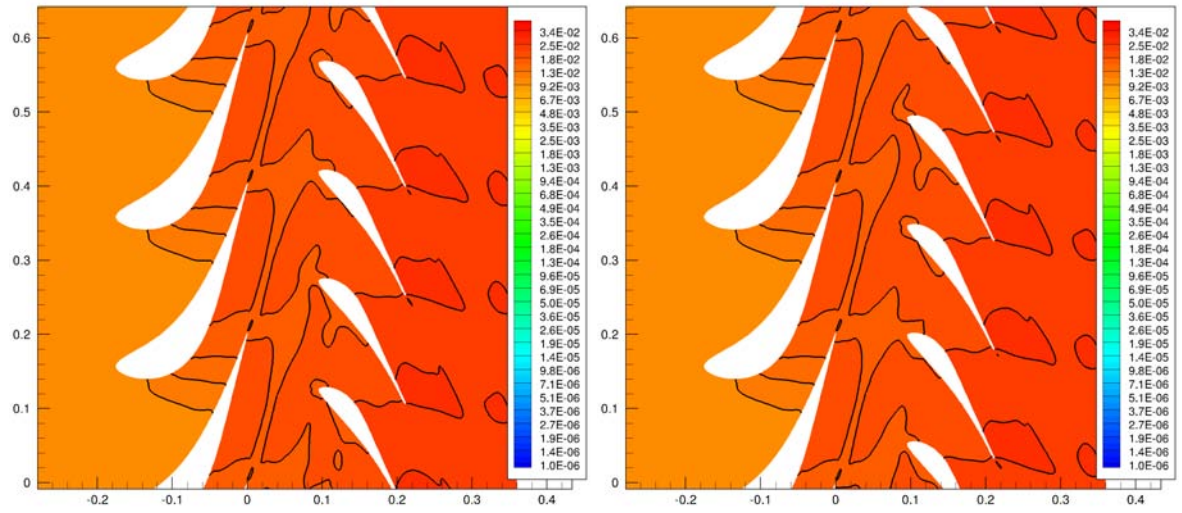

(a) $t = t_0$, case 2 (b) $t = t_0 + 0.5\tau_R$, case 2

Fig. 8: Average droplet size $[\mu m]$.

References

Becker, R., Döring, W. (1935), Kinetische Behandlung der Keimbildung in übersättingten Dämpfen. *Journal Ann. d. Physik*, Vol. 24, No. 8.

Petr, V., Kolovratník, M. (2001), Heterogenous Effects in the Droplet Nucleation Process in LP Steam Turbines, *4th European Conference on Turbomachinery*, Firenze.

Hill, P. G. (1966), Condensation of water vapor during supersonic expansion in nozzles, part 3, *Journal of Fluid Mechanics*, Vol.3, 593–620.

Strang, G., (1968), On the construction and comparison of difference schemes, *SIAM Journal of Numerical Analysis*, Vol. 5, 506–517.

Barschdorff, D., (1971), Verlauf der Zustandgroesen und gasdynamische Zuammenhaenge der spontanen Kondensation reinen Wasserdampfes in Lavalduesen, *Forsch. Ing.-Wes.*, Vol. 37, No. 5, (in german).

Dykas, S., Goodheart, K., Schnerr, G.H., (2003), Numerical study of accurate and efficient modeling for simulation of condensing flow in transonic steam turbines, *5th European conference on Turbomachinery*, Prague, 751–760.

Young, J.B., (1992), Two-Dimensional, Nonequilibrium, Wet–Steam Calculations for Nozzles and Turbine Cascades, *Journal of Turbomachinery*, vol 114.

Šejna, M., Lain, J. (1994), Numerical modelling of wet steam flow with homogenous condensation on unstructured triangular meshes, *Journal ZAMM*, vol. 74, no. 5, 375–378.

Šťastný, M., Šejna, M., (1995), Condensation effects in transonic flow through turbine cascade, *Proceedings of the 12th international conference of the properties of water and steam*, Begel House, 711–719.

, Sopuch P., (1996), Kinetics of phase change vapor-liquid and its numerical simulation, *Doctoral thesis*, IT CAS CR, (in Czech).

Halama, J., Fořt, J., Seifert, M., (2010), Numerical solution of wet steam flow with a priori droplet size distribution, *Proceedings of Conference 'Topical Problems of Fluid Mechanics'*, Prague, 63–66.

Halama, J., Benkhaldoun, F., Fořt, J., (2011), Flux schemes based finite volume method for internal transonic flow with condensation, *International Journal for Numerical Methods in Fluids*, vol. 65, no. 8, 953–968.